Improved Gaussian Process Modelling of On-Axis and Off-Axis Monostatic RCS Magnitude Responses of Shoulder-Launched Missiles

Warren P. du Plessis and Jan P. Jacobs

Department of Electrical, Electronic and Computer Engineering
University of Pretoria, Hatfield, 0028, South Africa
jpjacobs@up.ac.za, wduplessis@ieee.org

Abstract ─ An improved Gaussian-process-based technique is described for modelling both on-axis and off-axis monostatic RCS magnitude responses of shoulder-launched missiles. The RCS responses are complicated, oscillatory, quasi-periodic functions of frequency, with the oscillation periods being related to the spacings of the scatterers comprising the missiles. The updated modelling approach employs a spectral-mixture covariance function, whose components explicitly include distinct oscillations. The proposed technique is evaluated by means of two example missiles. For the six rotations considered, average predictive normalised RMSE ranged from 0.34% to 0.87% and from 0.95% to 1.53% for the two missiles respectively.

Index Terms ─ Gaussian processes, modelling, radar cross-section.

I. INTRODUCTION

A radar system has little or no influence over the radar cross-section (RCS) of a target [1, 2], making RCS the driving factor behind a variety of radar design decisions (e.g., [2, 3]). RCS magnitude strongly affects radar performance via SNR, and influences countermeasure performance via the jammer-to-signal ratio (JSR) [2].

The majority of radar targets have dimensions which are significantly larger than a wavelength, so RCS simulations normally require vast quantities of memory and take a long time, even when high-frequency techniques such as physical optics (PO) are used. Unfortunately, the fact that radar targets are so much larger than the wavelength means that the RCS magnitude varies rapidly with frequency and rotation [1], so RCS must be determined at a large number of frequencies and rotations. Accurately modelling RCS magnitude as a function of frequency would reduce the number of frequency points at which RCS must be determined (e.g., via costly simulations), thereby reducing the time required to reliably obtain platform RCS.

Despite the clear value of RCS magnitude modelling, it has received surprisingly little attention in the literature (studies concerned with modelling RCS magnitude as a function of frequency include [4-10]), and in most cases, the targets considered either have very specific attributes (e.g., strong resonances), have simpler responses than the missiles considered here, or only consider angular interpolation. There is a relatively large body of literature which attempts to extract accurate models of targets from RCS responses (e.g., [11-14]), but the emphasis in these studies is on target characterisation rather than RCS modelling. There is thus a need to consider the modelling of RCS responses of realistic targets, like missiles.

It has recently been demonstrated that Gaussian process (GP) regression [15] can be used to create accurate models of monostatic RCS magnitude responses of shoulder-launched missiles [10]. Integral to the models was the use of a specially constructed composite covariance function formed by taking the product of standard squared-exponential and periodic covariance functions [15]. It was shown that GP regression outperformed support vector regression, a GTD-based approximation technique, and spline interpolation in modelling the highly oscillatory RCS magnitude responses of Stinger and Strela missile models. GP regression has also been used in conjunction with a Bayesian committee machine to model RCS responses as a function of object shape [16], further demonstrating the value of the GP approach to RCS modelling. However, these investigations did not consider RCS frequency response [16]. Furthermore, similar to [10], only frontal-incidence (on-axis) RCS responses were considered.

In the present study, the technique described in [10] is extended to account for monostatic RCS responses involving an additional missile type, as well as different angles of incidence (i.e., off-axis). These challenging additional test cases expose limitations of the composite SE×PER covariance function used previously [10]. The structure of the frequency response of the RCS magnitude suggests that using a spectral-mixture covariance function [17] (not previously used for

Submitted On: May 26, 2019
Accepted On: August 11, 2019

electromagnetic modelling) will produce better results, and experimental results confirm that this is indeed the case.

II. GAUSSIAN PROCESS MODELLING

The goal is to model the response of the RCS magnitude as a function of frequency, i.e., a one-dimensional latent function that is assumed to be noise-free.

Consider a training set $\{(x_i, g_i) \mid i = 1, \ldots, n\}$ consisting of observations of the latent function, where the inputs x_i and outputs (targets) g_i are frequency and RCS magnitude respectively. In order to make predictions at new (test) inputs $\{x_{*,j} \mid j = 1, \ldots, n_*\}$, the first step is to define a jointly Gaussian prior distribution over the n training outputs (vector $\mathbf{g}$) and the n_* unknown test outputs (vector $\mathbf{g}_*$) [15]:

$$\begin{bmatrix} \mathbf{g} \\ \mathbf{g}_* \end{bmatrix} \sim \mathcal{N}\left(\mathbf{0}, \begin{bmatrix} K(\mathbf{x},\mathbf{x}) & K(\mathbf{x},\mathbf{x}_*) \\ K(\mathbf{x}_*,\mathbf{x}) & K(\mathbf{x}_*,\mathbf{x}_*) \end{bmatrix} \right), \quad (1)$$

where $\mathcal{N}(\mathbf{u}, V)$ denotes a multivariate normal distribution with mean vector $\mathbf{u}$ and covariance matrix V, while $\mathbf{x}$ and $\mathbf{x}_*$ are vectors containing the training and test inputs respectively. The shape of the prior is determined by the covariance matrix with sub-matrices $K(\cdot)$, where for example, $K(\mathbf{x}, \mathbf{x}_*)$ is an $n \times n_*$ covariance matrix holding the covariances between all pairs of training and test outputs, and the remaining $K(\cdot)$ are similarly defined.

Elements of the covariance matrices in (1) are given by a covariance function $k(x, x')$, which gives the covariance between the values of the process at x and x'. A popular standard covariance function which is frequently used for antenna modelling [18] is the squared-exponential (SE) covariance function:

$$k_{\text{SE}}(x, x') = \sigma_f^2 \exp\left[-0.5 \left(\frac{x - x'}{\tau} \right)^2 \right], \quad (2)$$

where σ_f^2 is a parameter that governs the variance of the process and τ is a positive length-scale parameter [15]. To make predictions, it is required that a posterior distribution be constructed by conditioning the test outputs $\mathbf{g}_*$ on the known training outputs $\mathbf{g}$; the posterior is given by $\mathbf{g}_* \mid \mathbf{x}_*, \mathbf{x}, \mathbf{g} \sim \mathcal{N}(\mathbf{m}, \Sigma)$ [15]. The mean $\mathbf{m}$ of the posterior is given by,

$$\mathbf{m} = K(\mathbf{x}_*, \mathbf{x}) K(\mathbf{x}, \mathbf{x})^{-1} \mathbf{g}, \quad (3)$$

and contains the most likely RCS magnitudes at the test frequencies in $\mathbf{x}_*$. Alternatively, the prediction at a point x_* may be expressed in terms of a sum of weighted covariance functions placed at the training points [15]:

$$m_* = m(x_*) = \sum_{i=1}^{n} \alpha_i k(x_i, x_*), \quad (4)$$

where vector $\alpha = K(\mathbf{x}, \mathbf{x})^{-1} \mathbf{g}$, and $k(x_i, x_*)$ is the covariance function situated at training point x_i. The hyperparameters of the covariance function (e.g., σ_f^2 and τ in (4)) are optimised during training, which involves minimising the negative log marginal likelihood with respect to the hyperparameters [15, eq. (2.29)].

Used by itself, the above-mentioned SE covariance function is incapable of accurately modelling oscillatory responses of shoulder-launched missiles such as those shown below in Figs. 2 and 3. Previously [10], this difficulty was addressed by combining the SE covariance function, k_{SE}, with the standard periodic covariance function, k_{PER}, given by [15]:

$$k_{\text{PER}}(x, x') = \exp\left[-\frac{2}{\theta^2} \sin^2\left(\pi \frac{x - x'}{\lambda} \right) \right], \quad (5)$$

where the intervals between repetitions are determined by λ, while θ is a length-scale parameter. The resulting composite covariance function is given by [10]:

$$k_{\text{SE}\times\text{PER}} = k_{\text{SE}} \times k_{\text{PER}}, \quad (6)$$

$$= \sigma_f^2 \exp\left[-0.5 \left(\frac{x - x'}{\tau} \right)^2 \right] \times \exp\left[-\frac{2}{\theta^2} \sin^2\left(\pi \frac{x - x'}{\lambda} \right) \right], \quad (7)$$

which has four hyperparameters, σ_f τ, θ, and λ. While the results obtained using $k_{\text{SE}\times\text{PER}}$ for models of the Strela and Stinger missiles for front-on incidence were good [10], it is demonstrated in Section III below that predictive performance was significantly poorer when extended to rotated versions of the Strela as well as an Igla missile (front-on incidence and rotations).

The RCS responses of shoulder-launched missiles are intricate, oscillatory, quasi-periodic functions of frequency. In physics-based approaches to calculating RCS response approximations, the target is often modeled as a collection of point scatterers placed at defining structural positions of the target [1]. This approach leads to a model comprising sinusoidal oscillations whose periods are related to the spacings of the scatterers (see (1) below). Broadly speaking, the notion that multiple periods need to be taken into account suggests that a covariance function that explicitly allows multiple distinct sinusoidal oscillations might be a better modelling tool than $k_{\text{SE}\times\text{PER}}$ for RCS responses such as those shown in Fig. 3.

The spectral mixture (SM) covariance function, k_{SM} [17] is such a covariance function. For one-dimensional inputs, k_{SM} can be expressed as [17]:

$$k_{\mathrm{SM}}\left(x,x'\right)=\sum_{q=1}^{Q}w_q^2\,\exp\left[-2\pi\sigma_q^2\left(x-x'\right)^2\right]\times \cos\left[2\pi\mu_q\left(x-x'\right)\right], \tag{8}$$

where Q is the number of spectral mixtures, and the hyperparameters w_q, μ_q, and σ_q^2 are respectively the weight, mean, and variance of the Gaussians comprising the qth mixture. This nomenclature arises as Bochner's theorem allows k_{SM} to be interpreted as the inverse Fourier transform of the sum of Q scale-location Gaussian spectral density mixtures, with each mixture containing two Gaussians centered symmetrically about the spectral origin [15, 17]. By comparison, the SE covariance function is the inverse Fourier transform of only a single Gaussian spectral density centered at the origin. The number of hyperparameters to be optimised for k_{SM} is $3Q$, compared to four hyperparameters for $k_{\mathrm{SE\times PER}}$ used in [10].

In Section III, it is demonstrated that GP regression using k_{SM} gives very accurate results, significantly improving on those obtained using GP regression with $k_{\mathrm{SE\times PER}}$. It was previously demonstrated that the point-scatterer concept in the form of a GTD-based approach was significantly less accurate than GP regression employing $k_{\mathrm{SE\times PER}}$ in modelling the front-on RCS responses of missiles [10]. Tables 1 and 2 below show that k_{SM} in turn outperformed $k_{\mathrm{SE\times PER}}$ for all rotations (including front-on incidence) of the Strela and Igla missiles considered. The apparent accuracy difference (k_{SM} versus point-scatterer concept) is perhaps surprising in light of the fact that both k_{SM} and the point-scatterer model make use of a number of sinusoidal terms with differing periods. It is therefore informative to compare the GP regression using k_{SM} in (3) after training to the point-scatterer view.

Under the latter approach, the reflections from the scatterers are combined with phase shifts which depend on the distances between the scatterers from the perspective of a radar, giving an RCS magnitude of,

$$\mathrm{RCS}\quad\approx\left|\sum_{i=1}^{S}a_i e^{j\phi_i}e^{j\beta d_i}\right|^2, \tag{9}$$

where S is the number of scatterers, each with magnitude a_i, phase φ_i, and position d_i, with $\beta=2\pi f/c$ being the propagation phase constant where f is the frequency and c is the propagation velocity. It can be shown that the RHS of (9) reduces to:

$$\mathrm{RCS}\quad\approx\sum_{i=1}^{S}\sum_{j=1}^{S}k_{1ij}\cos\left[k_{2ij}+k_{3ij}\left(d_i-d_j\right)f\right], \tag{10}$$

where k_{nij}, n=1, 2, 3 are constants. In other words, (1) approximates the RCS magnitude by a sum of sinusoidal functions of frequency. Each term takes effect over the whole frequency range (e.g., 5 to 15 GHz in Fig. 3), which suggests limited flexibility compared to the use of k_{SM} in (8). The summed, weighted multiple frequency components of k_{SM} (i.e., the mixtures) fulfil a similar role to that of basis functions (see (4)), but only have a significant effect in the vicinity of the training points they are placed at due to the decaying squared exponential component of k_{SM}. The placement of multiple mixtures locally at each training point makes GP regression using k_{SM} in (3) far more powerful than the point-source approximation in (1) despite the apparent similarity of these two models.

III. VERIFICATION EXAMPLES

Models of the F9K32 Strela-2 (SA-7 Grail) and Igla-S (SA-24 Grinch) missiles constructed from information freely available on the internet are shown in Fig. 1.[1]

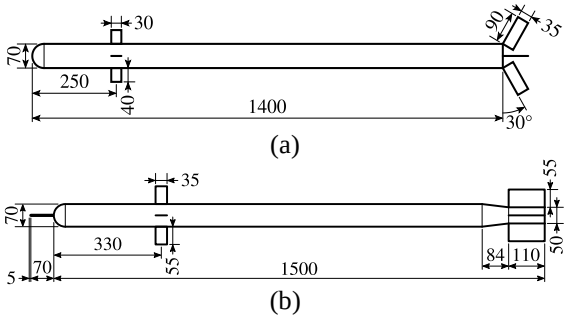

Fig. 1. The dimensions of: (a) Strela and (b) Igla missile models in mm.

FEKO release 2017.1 [19] was used to establish the ground truth data with 501 frequencies being simulated from 5 to 15 GHz (20-MHz steps) per missile using the method of moments (MoM) solver with default settings. Simulations included frontal on-axis incidence (defined as the 0° rotation), as well as incidence at rotations of 3°, 6°, 9°, 12°, and 15° in the horizontal plane measured relative to the missile axis from the front. This angular range covers hypothetical cases with the target ranging from a hovering helicopter (0°) to a cruising propellor-driven transport aircraft (15°). The incident wave was horizontally polarised, and the horizontal component of the reflected wave was considered for the RCS calculation.

Simulation run times and memory requirements were reduced by using electrical and magnetic symmetry where applicable. Maximum triangle edge lengths of a tenth of a wavelength were used, and further run-time reduction was achieved by generating separate meshes at each frequency. It was not possible to use high-frequency techniques such as PO as the main features

[1] The Igla proved more challenging to model than the Stinger considered in [10] and was thus used instead. For example, for front-on incidence the SE×PER function yielded a mean RMSE of 7.27% for the Igla (see Table 2) versus 1.24% for the Stinger [10].

are smaller than five wavelengths even at the highest frequencies [1]. A maximum of 285 GB of memory and a grand total of 670 hours of simulation time were required to simulate the two missiles, despite the small target sizes. Each simulation used a cluster of five computers, each with a minimum of 64 GB of memory and two 12-core Intel Xeon E5-2690 v3 processors running at 2.60 GHz.

Twenty sets of training data points (subsets of the ground truth simulation data) were compiled for each missile to verify that results were independent of specific configurations of training points [10]. To ensure that input frequency points were spread over the entire frequency range rather than being clumped together (cf. Fig. 3), the interval of 5 to 15 GHz was divided into equal sub-intervals, and one frequency point was uniformly randomly selected from each of these sub-intervals. The extreme frequency values (5 and 15 GHz) were then added if not yet present, giving a total of about 166 (Strela) or 168 (Igla) points.

A frequency step of 50 MHz or less is necessary to ensure that 1.5-m separation of the nose and tail of a missile can be resolved by the RCS magnitude [1, 10]. However, this estimate is somewhat optimistic as the nose-to-tail distance decreases with rotation, and interactions between other features of a target (e.g., the missile wings in Fig. 1) can produce variations over smaller frequency ranges. The use of 166 to 168 points is thus significantly lower than the estimated 201 required points.

Training consisted of gradient-based optimisation of the negative log marginal likelihood [15, eq. (2.29)], which is highly multi-modal. This necessitated considering multiple sets of hyperparameter starting values to ensure satisfactory results [10, 20]. For the spectral mixture covariance function in (8), a choice of $Q = 3$ mixtures gave a good compromise between flexibility and time required to optimise the hyperparameters. Experiments revealed that 750 sets of initial hyperparameter sets reliably gave satisfactory results for all runs; i.e. the hyperparameter set with the lowest negative log-likelihood always gave the best predictions, suggesting that model selection was robust.

Initial values of hyperparameters in (8) were selected according to a procedure suggested in [20]. The weights w_q, where $q = 1, ..., Q$, were set equal to the standard deviation of the training targets (i.e., simulated RCS magnitude values) divided by the number of mixtures Q. The repetition rates μ_q were uniformly randomly selected from a range which had zero as lower bound, and an upper bound that was proportional to the reciprocal of the smallest frequency spacing between the randomly-selected training points. The hyperparameters σ_q are the inverse length scales of the squared exponentrial constituent functions in (8). The initial length scales were taken to be the absolute values of random numbers drawn from a zero-mean normal distribution that had a standard deviation that was equal to the overall range of the training data (length scales are defined as positive). It is worth noting that the length scale parameters σ_q determine the effective range of frequencies which are affected by each term of (8) for each training point.

The longest per-run training times was on the order of 60 minutes, which is far lower than the FEKO simulation time. For the SE×PER covariance function with four unknown hyperparameters, 300 sets of random starting values were used as a larger number did not improve results. Results for the hyperparameter sets with the lowest negative log-likelihood are reported below.

The errors obtained by each model were quantified using the normalised RMSE defined by:

$$\mathrm{RMSE} = \frac{\sqrt{\frac{1}{n_*}\sum_{l=1}^{n_*}\left[\mathrm{RCS}_p(l) - \mathrm{RCS}_s(l)\right]^2}}{\max_l\left[\mathrm{RCS}_s(l)\right] - \min_l\left[\mathrm{RCS}_s(l)\right]}, \qquad (11)$$

where the predicted and simulated linear RCS magnitudes at frequencies l are denoted $\mathrm{RCS}_p(l)$ and $\mathrm{RCS}_s(l)$ respectively. The results reported below only consider the test points (i.e., the subsets of the 501 available points remaining after the training points were removed) as the errors at the training points are negligible for GP regression with noise-free observations.

Tables 1 and 2 provide RMSE statistics for 20 runs of GP regression with the SE×PER and SM3 (SM with three mixtures) covariance functions for the Strela and Igla missiles, respectively.

The importance of considering different rotations is demonstrated by the fact that the most accurate results for the Strela in Table 1 are obtained when the rotation is small. However, these missiles may approach their targets at larger rotations, so errors in the RCS magnitude need to be small over the full range of rotations which will be encountered in practice.

The importance of considering different rotations is demonstrated by the fact that the most accurate results for the Strela in Table 1 are obtained when the rotation is small. However, these missiles may approach their targets at larger rotations, so errors in the RCS magnitude need to be small over the full range of rotations which will be encountered in practice.

The results in Table 1 indicate that both covariance functions provide accurate results for the Strela, with SM3 reducing the mean RMSE obtained by SE×PER by 50% or more for most rotations. The situation changes dramatically for the Igla in Table 2, where the accuracy of SM3 is considerably better than SE×PER, with mean RMSE varying from 3.26% to 7.27% for SE×PER and from 0.95% to 1.53% for SM3.

Tables 1 and 2 also show that SE×PER performance was more strongly influenced by the training data configurations associated with particular runs than SM3.

For example, the RMSEs at a 9° rotation varied from 0.83% to 5.17% for SE×PER versus 0.23% to 1.71% for SM3 in Table 1, and from 2.14% to 6.82% for SE×PER and from 0.37% to 3.59% for SM3 in Table 2.

Figure 2 compares SE×PER and SM3 predictive responses for the Strela missile at 9° rotation for a particular training data configuration (i.e., the same training points were used in both cases). For this run, the random selection of training points in the region 5 to 5.5 GHz produced no points at consecutive response maxima, which causes substantial inaccuracies in the SE×PER predictions. On the other hand, the expressive power of the SM3 covariance function allows the regression to infer the underlying response structure more effectively, yielding significantly better predictions over this range in spite of the unfavourably placed training points.

Figure 3 provides results for the Igla missile at 12° rotation that are representative of the GP models' mean predictive performance (i.e., the solution with the RMSE closest to the mean is shown in each case). While the SE×PER model follows the simulated response reasonably well, there are several frequencies with large errors, and some predictions even have negative values, which are not physically possible. Comparing the SE×PER and SM3 models in Fig. 3 clearly demonstrates the superior performance of SM3, which has both fewer and smaller significant deviations from the simulated response.

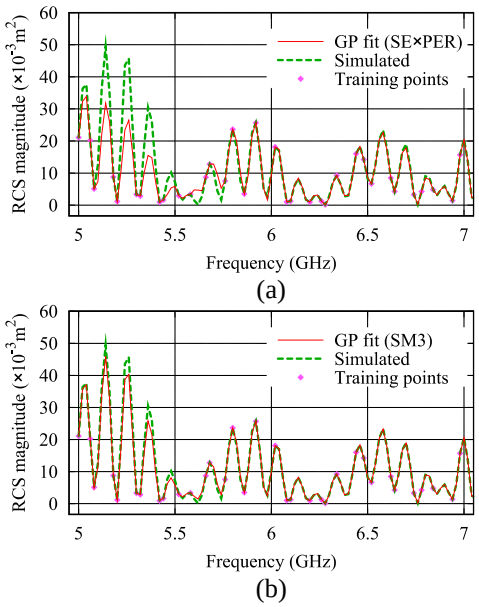

Fig. 2. GP predictive results for the Strela missile at 9° rotation using: (a) SE×PER (RMSE = 5.17%), and (b) SM3 (RMSE = 1.42%) covariance functions, compared to the simulated (true) RCS magnitude. Only the lower 2 GHz of the 10-GHz range is shown as errors over the remainder of the frequency range are negligible.

Table 1: RMSEs of Strela test data

Cov.	Rot. Func.	Mean	Best	Median	Worst
SE×PER	0°	0.93%	0.66%	0.88%	1.57%
	3°	0.74%	0.50%	0.71%	1.46%
	6°	1.07%	0.63%	0.97%	2.02%
	9°	1.83%	0.83%	1.41%	5.17%
	12°	1.80%	1.00%	1.73%	3.55%
	15°	1.10%	0.45%	0.98%	3.29%
SM3	0°	0.49%	0.19%	0.49%	1.12%
	3°	0.34%	0.15%	0.30%	0.64%
	6°	0.52%	0.20%	0.45%	1.11%
	9°	0.87%	0.23%	0.75%	1.71%
	12°	0.86%	0.46%	0.64%	1.90%
	15°	0.81%	0.25%	0.62%	2.43%

Table 2: RMSEs of Igla test data

Cov.	Rot. Func.	Mean	Best	Median	Worst
SE×PER	0°	7.27%	3.94%	7.63%	10.08%
	3°	5.68%	3.09%	5.97%	7.66%
	6°	3.26%	1.94%	3.10%	5.11%
	9°	3.71%	2.14%	3.22%	6.82%
	12°	6.35%	5.12%	6.47%	7.96%
	15°	4.96%	2.78%	5.09%	7.50%
SM3	0°	1.33%	0.52%	1.20%	2.37%
	3°	0.95%	0.37%	0.87%	1.86%
	6°	1.08%	0.64%	1.00%	1.79%
	9°	1.32%	0.37%	1.18%	3.59%
	12°	1.53%	0.65%	1.29%	3.31%
	15°	1.35%	0.51%	1.25%	2.82%

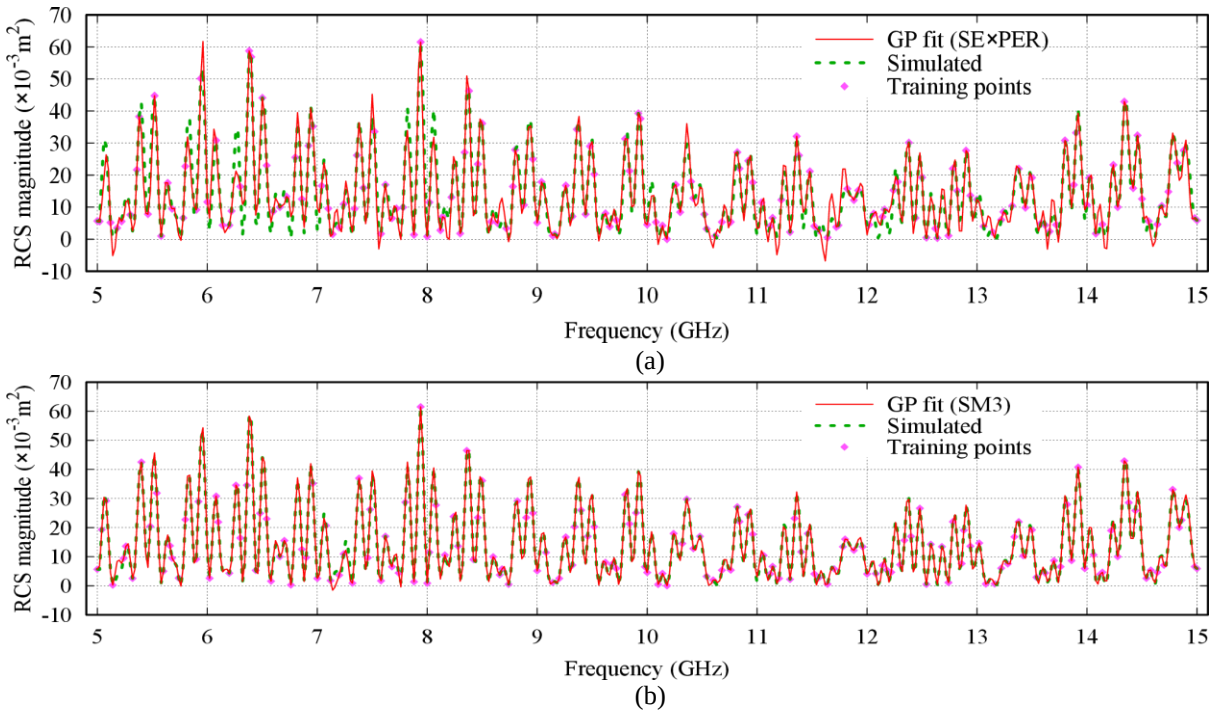

Fig. 3. Typical GP predictive results for the Igla missile at 12° rotation using: (a) SE×PER (RMSE = 6.35%), and (b) SM3 (RMSE = 1.50%) covariance functions, compared to the simulated (true) RCS magnitude.

VI. CONCLUSION

GP regression with an SM covariance function was used to model RCS magnitude responses of shoulder-launched missiles. The SM covariance function was selected since its constituent functions render it sufficiently flexible to account for oscillatory responses such as those shown in Figs. 2 and 3. Even using only three mixtures, the SM covariance function was demonstrated to yield very high predictive accuracies for all missiles and angles of incidence considered, significantly improving on results previously obtained for the same problem using a hybrid SE×PER covariance function. It was further shown that successful gradient-based optimisation of the covariance function hyperparameters could be carried out in spite of a severely multimodal negative log-likelihood function for the data considered. Significantly, the accuracy of the predictive results was shown to be almost independent of the configuration of the training points used.

ACKNOWLEDGMENT

This work is based on the research supported in part by the NRF (Grant Numbers 103855 and 119151). The authors acknowledge the Centre for High Performance Computing, South Africa, for providing computational resources to this research project.

REFERENCES

[1] E. Knott, J. Schaeffer, and M. Tulley, *Radar Cross Section*. SciTech, Rayleigh, NC, Second ed., 2004.

[2] G. W. Stimson, H. D. Griffiths, C. J. Baker, and D. Adamy, *Stimson's Introduction to Airborne Radar*. SciTech, Edison, NJ, Third ed., 2014.

[3] A. A. Black, "Pulse doppler for missile approach warning," *J. Electron. Defence (JED)*, vol. 14, no. 8, pp. 44-52, Aug. 1991.

[4] J. Yang and T. K. Sarkar, "Interpolation/extrapolation of radar cross-section (RCS) data in the frequency domain using the Cauchy method," *IEEE Trans. Antennas Propag.*, vol. 55, no. 10, pp. 2844-2851, Oct. 2007.

[5] L. de Tommasi, B. Gustavsen, and T. Dhaene, "Accurate macromodeling Based on Tabulated Magnitude Frequency Responses," in *2008 12th IEEE Workshop on Signal Propagation on Interconnects*, pp. 1-4, May 2008.

[6] J. Yang, M. C. Taylor, Y. Zhang, and T. K. Sarkar, "Efficient interpolation of high-frequency domain data by phase smoothing," *Radio Sci.*, vol. 43, no. 04, pp. 1-15, Aug. 2008.

[7] B. Persson and M. Norsell, "On modeling RCS of aircraft for flight simulation," *IEEE Antennas Propag. Mag.*, vol. 56, no. 4, pp. 34-43, Aug. 2014.

[8] Y. Yang, Y. Ma, and L. Wang, "The simultaneous interpolation of target radar cross section in both the spatial and frequency domains by means of Legendre wavelets model-based parameter estimation," *Int. J. Aerospace Eng.*, vol. 2015,

2015.
[9] J. Yang and T. K. Sarkar, "Accurate interpolation of amplitude-only frequency domain response based on an adaptive Cauchy method," *IEEE Trans. Antennas Propag.*, vol. 64, no. 3, pp. 1005-1013, Mar. 2016.
[10] J. P. Jacobs and W. P. du Plessis, "Efficient modeling of missile RCS magnitude responses by Gaussian processes," *IEEE Antennas Wireless Propag. Lett.*, vol. 16, pp. 3228-3231, Nov. 2017.
[11] R. Carrière and R. L. Moses, "High resolution radar target modeling using a modified Prony estimator," *IEEE Trans. Antennas Propag.*, vol. 40, no. 1, pp. 13-18, Jan. 1992.
[12] L. C. Potter, D.-M. Chiang, R. Carriere, and M. J. Gerry, "A GTD-based parametric model for radar scattering," *IEEE Trans. Antennas Propag*., vol. 43, no. 10, pp. 1058-1067, Oct. 1995.
[13] M. J. Gerry, L. C. Potter, I. J. Gupta, and A. Van Der Merwe, "A parametric model for synthetic aperture radar measurements," *IEEE Transactions on Antennas and Propagation*, vol. 47, no. 7, pp. 1179-1188, July 1999.
[14] W. Lee, T. K. Sarkar, H. Moon, and M. Salazar-Palma, "Computation of the natural poles of an object in the frequency domain using the Cauchy method," *IEEE Antennas Wireless Propag. Lett.*, vol. 11, pp. 1137-1140, 2012.
[15] C. E. Rasmussen and C. K. I. Williams, *Gaussian Processes for Machine Learning*. MIT Press, Cambridge, MA, 2006.
[16] K. Wang, D. Ding, and R. Chen, "A surrogate modeling technique for electromagnetic scattering analysis of 3-D objects with varying shape," *IEEE Antennas Wireless Propag. Lett.*, vol. 17, no. 8, pp. 1524-1527, 2018.
[17] A. G. Wilson, E. Gilboa, A. Nehorai, and J. P. Cunningham, "GPatt: Fast multidimensional pattern extrapolation with Gaussian processes," *arXiv preprint arXiv:1310.5288*, 2013.
[18] J. P. Jacobs and S. Koziel, "Two-stage framework for efficient Gaussian process modeling of antenna input characteristics," *IEEE Trans. Antennas Propag.*, vol. 62, no. 2, pp. 706-713, Feb. 2014.
[19] Altair Hyperworks, *FEKO User Manual*, 2017.
[20] A. G. Wilson, "Scalable kernel learning and Gaussian processes – Spectral mixture kernels," https://people.orie.cornell.edu/andrew/pattern/#spectral, Oct. 2018.

Warren P. du Plessis received the B.Eng. (Electronic) and M.Eng. (Electronic) and Ph.D. (Engineering) degrees from the University of Pretoria in 1998, 2003, and 2010 respectively, winning numerous academic awards including the prestigious Vice-Chancellor and Principal's Medal.

He spent two years as a Lecturer at the University of Pretoria, and then joined Grintek Antennas as a Design Engineer for almost four years, followed by six years at the CSIR. He is currently a Professor at the University of Pretoria, and his primary research interests are cross-eye jamming and thinned antenna arrays.

Jan Pieter Jacobs received the B.Eng., M.Eng., and Ph.D. degrees in Electronic Engineering from the University of Pretoria, Pretoria, South Africa, and a doctorate in Music from Yale University, New Haven, CT, USA.

He is a registered Professional Engineer in South Africa and is an Associate Professor in the Department of Electrical, Electronic and Computer Engineering at the University of Pretoria. His research interests include modelling and optimization of microwave antennas and devices, computational electromagnetics, slot antennas and arrays, and pattern recognition in music.